Journal of Energy Chemistry 34 (2019) 52–56

Contents lists available at ScienceDirect

Journal of Energy Chemistry

journal homepage: www.elsevier.com/locate/jechem

http://www.journals.elsevier.com/journal-of-energy-chemistry/

A bipolar verdazyl radical for a symmetric all-organic redox flow-type battery

Grant D. Charlton[a], Stephanie M. Barbon[b], Joe B. Gilroy[b,*], C. Adam Dyker[a,*]

[a] Department of Chemistry, University of New Brunswick, Fredericton E3B 5A3, New Brunswick, Canada
[b] Department of Chemistry and the Centre for Advanced Materials and Biomaterials Research (CAMBR), The University of Western Ontario, London N6A 5B7, Ontario, Canada

ARTICLE INFO

Article history:
Received 29 August 2018
Revised 27 September 2018
Accepted 29 September 2018
Available online 18 October 2018

Keywords:
All-organic redox flow battery
Energy storage
Verdazyl radicals
Organic radical
Coin cell

ABSTRACT

A symmetric all-organic non-aqueous redox flow-type battery was investigated employing the neutral small molecule radical 3-phenyl-1,5-di-*p*-tolylverdazyl, which can be reversibly oxidized and reduced in one-electron processes, as the sole charge storage material. Cyclic voltammetry of the verdazyl radical in 0.5 M tetrabutylammonium hexafluorophosphate ($TBAPF_6$) in acetonitrile revealed redox couples at – 0.17 V and – 1.15 V vs. Ag^+/Ag, leading to a theoretical cell voltage of 0.98 V. From the dependence of peak currents on the square root of the scan rate, diffusion coefficients on the order of 4×10^{-6} cm^2 s^{-1} were demonstrated. Cycling performance was assessed in a static cell employing a Tokoyuma AHA anion exchange membrane, with 0.04 M verdazyl as catholyte and anolyte in 0.5 M $TBAPF_6$ in acetonitrile at a current density of 0.12 mA cm^{-2}. Although coulombic efficiencies were good (94%–97%) throughout the experiment, the capacity faded gradually from high initial values of 93% of the theoretical discharge capacity to 35% by the 50th cycle. Voltage and energy efficiencies were 68% and 65%, respectively. Post-cycling analysis by cyclic voltammetry revealed that decomposition of the active material with cycling is a leading cause of cell degradation.

1. Introduction

Redox flow batteries (RFBs) are a promising large scale energy storage solution for integrating renewable energy, such as from solar, wind, or other sources, with electrical grids [1–6]. The active anode and cathode materials in RFBs are each dissolved in the electrolyte (anolyte and catholyte, respectively) and stored in separate tanks, and then pumped into the electrochemical cell for charging/discharging. One of the major advantages of RFBs over other energy storage technologies is their scalability of design, in that the tank size can be increased or decreased to meet any capacity requirements, and the cell can be independently designed to meet power requirements. The most well studied class of RFB is that based on aqueous electrolytes [7,8], including the vanadium redox flow battery [9,10] which employs the VO_2^+/VO^{2+} couple as catholyte and the V^{3+}/V^{2+} couple as anolyte. Having both redox couples based on the same metal (vanadium) leads to the advantage of these cells not being susceptible to irreversible capacity loss caused by crossover of active material between the anolyte and catholyte. Nevertheless, as with all aqueous RFBs, the narrow cell voltage imposed by the electrolytic stability window for water limits energy densities. More recently, studies have been aimed at increasing energy densities by employing organic solvents (with stability windows up to ~5 V) to accommodate redox couples separated by larger potential gaps [11–13]. These include metal-based active materials, and all-organic systems. Organic active materials have the advantage of being tunable (to increase solubility, stability and/or redox potential) and offer the potential for low cost and environmentally friendly scalability compared to metal based systems which require environmentally intensive mining and processing [11–13].

Among the systems involving organic active materials, there have been a few recent studies employing a single active material, with three stable oxidation states, as both catholyte and anolyte. This includes nitronyl-nitroxides radicals (**A** and **B** in Fig. 1) [14,15], a diaminoanthraquinone (**C**) [16], and a benzoylpyridinium derivative (**D**) [17], as well as a dispersion (rather than a solution) of polythiophene (**E**) [18]. The Schubert group has also studied "combi-molecules" with two separate active sites, where a TEMPO cathode-active functional group has been tethered directly to phenazine (**F**) [19] or viologen (**G**) [20] as anode active species. Like vanadium RFBs, these symmetrical RFB designs have the ad-

* Corresponding authors.
E-mail addresses: joe.gilroy@uwo.ca (J.B. Gilroy), cadyker@unb.ca (C.A. Dyker).

https://doi.org/10.1016/j.jechem.2018.09.020

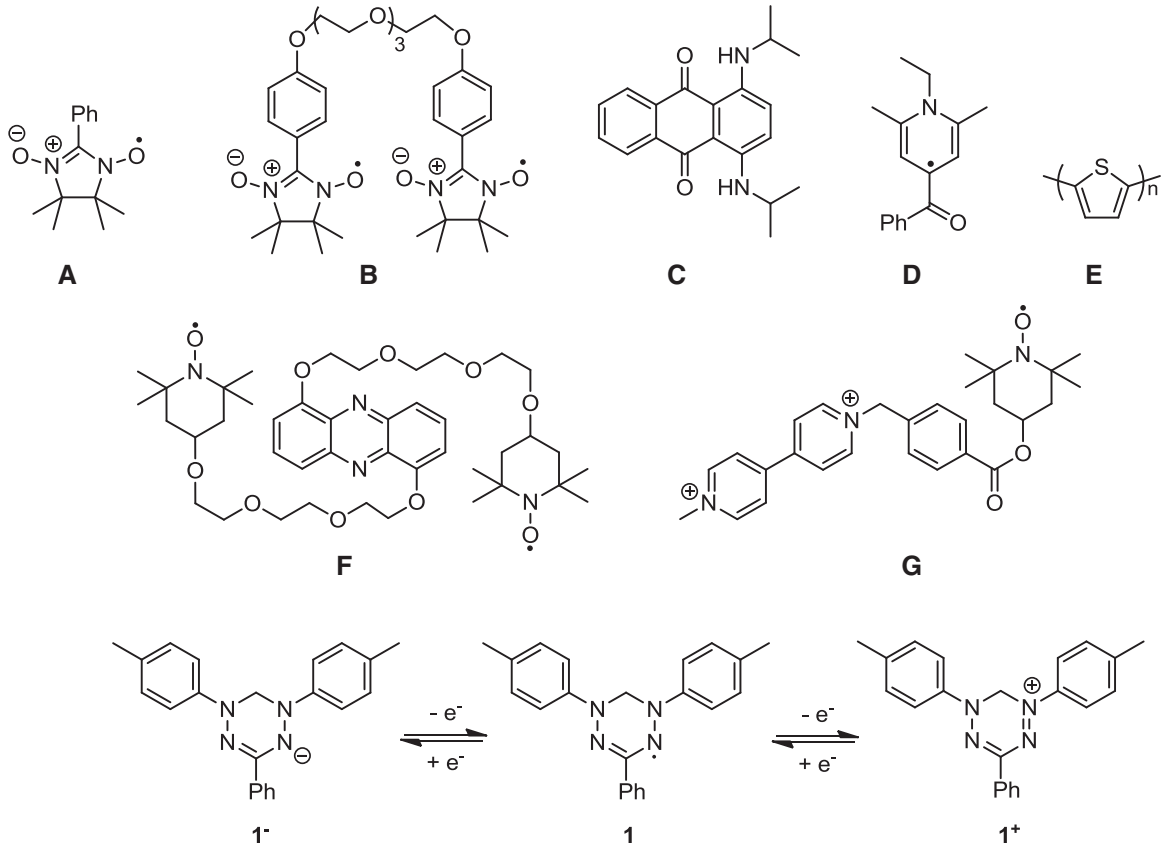

Fig. 1. Previously studied organic active materials for symmetrical RFBs (**A**–**G**), and the three stable oxidation states of 3-phenyl-1,5-di-*p*-tolylverdazyl (**1**).

vantage that crossover of active species does not irreversibly damage the cell, which is a major issue in designs involving distinct catholyte and anolyte materials. In order to expand on these studies, we now report an assessment of a verdazyl radical **1** (Fig. 1) as anode and cathode active species in a symmetrical redox flow-type battery.

2. Experimental

2.1. Chemicals

Acetonitrile was dried over calcium hydride and stored over 4 Å molecular sieves prior to use. Tetrabutylammonium hexafluorophosphate ($TBAPF_6$) was used as received from Aldrich. 3-Phenyl-1,5-di-*p*-tolylverdazyl (**1**) was prepared by a literature procedure [21].

2.2. Cyclic voltammetry

Cyclic voltammetry (CV) was carried out using potentiostat/galvanostat (BioLogic SP-150) with a cell which consisted of a working electrode (platinum disk, 0.07 cm^2), counter electrode (platinum wire, 5 cm) and Ag^+/Ag reference electrode (0.01 M $AgNO_3$ in 0.1 M $TBAPF_6$ in acetonitrile).

2.3. Cell design and testing

The electrolyte used in battery experiments was a 0.04 M solution of 3-phenyl-1,5-di-*p*-tolylverdazyl (**1**) in 0.5 M $TBAPF_6/CH_3CN$ as catholyte and anolyte. In order to simplify the evaluation of the energy storage characteristics of the organic active materials, a non-flowing configuration was chosen for this initial study. Thus the active material solutions and cell components were housed within two 2032 coin cell halves (MTI, two negative caps were used). In each half was placed a stainless steel spacer (∅ = 15.5 mm, MTI), and a piece of electrically conductive graphite felt (SGL Group, G334-01, dried under vacuum at 100 °C overnight prior to use; ∅ = 15 mm, electrode surface area = 1.77 cm^2). The cathodic and anodic graphite felts were soaked with 0.20 mL of the 0.04 M solution of **1**, respectively, so that the cell was initially assembled in the discharged state. A punched-out circular disc of 2.2 cm diameter (wider than the 2032 cell casings) of Tokuyama Neosepta AHA (0.20 mm thick) anionic exchange membrane (AEM, purchased from Electrolytica, USA, stored in 0.5 M aqueous NaCl) was used to separate the two half cells. The AEM was preconditioned by being soaked in the electrolyte (0.5 M $TBAPF_6$/acetonitrile) in the presence of molecular sieves at least 24 h prior to use. The whole cell was held together with a plastic coated pinch clamp, oriented vertically, and connected to the potentiostat/galvanostat (BioLogic SP-150). All CV and charge–discharge experiments were performed under argon atmosphere in a glove box with H_2O level ≤ 0.5 ppm and O_2 ≤ 1.0 ppm.

3. Results and discussion

3.1. Electrochemical characterization of *1*

The cyclic voltammetric analysis of a solution of compound **1** in 0.5 M $TBAPF_6/CH_3CN$ is shown in Fig. 2. The compound exhibited two separate one-electron redox couples at – 0.17 V ($\mathbf{1}^+/\mathbf{1}$) and – 1.15 V ($\mathbf{1}/\mathbf{1}^-$) vs Ag^+/Ag. In each case, the ratio of anodic and cathodic current peak heights was near unity (0.993 and 1.013, respectively) demonstrating good reversibility for each couple. In

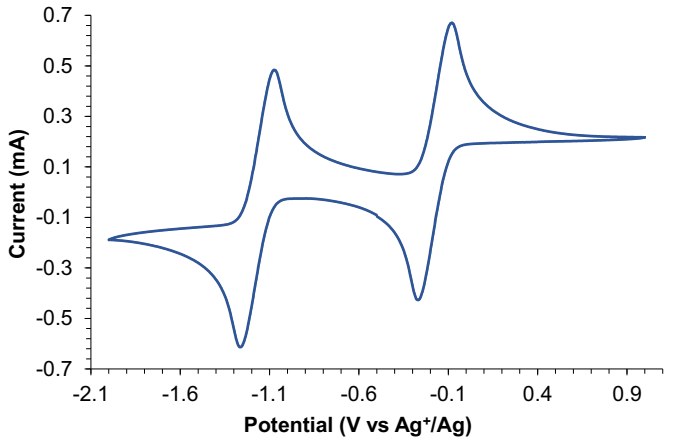

Fig. 2. The cyclic voltammogram of **1** in 0.5 M $TBAPF_6/CH_3CN$ at a scan rate of 100 mV s^{-1}, with a platinum working electrode, Ag^+/Ag reference electrode and a platinum wire counter electrode.

longer term CV cycling experiments (Fig. S1 in the Supplementary Information), the verdazyl radical demonstrated stability for over 100 sequential cycles, though current responses were observed to decrease by the 200th cycle.

Changes in peak current i_p (peak height) were measured as scan rates were varied from 10 to 160 mV s^{-1} for the 0.04 M **1**/0.5 M $TBAPF_6/CH_3CN$ solution, and the resulting CVs are shown in Fig. 3(a). A linear correlation between the square root of the scan rate and peak currents is shown in Fig. 3(b) and supports the chemical reversibility of the redox processes. The slopes of the plots can be related to the diffusion coefficients (D) through the Randles–Sevcik equation for a reversible redox couple, shown in Eq. (1) [22],

$$i_p = 2.69 \times 10^5 n^{3/2} A D^{1/2} C^* \nu^{1/2} \quad (1)$$

where i_p is the peak current in amperes, n is the number of electrons involved in the half-reaction for the redox couple, F is the Faraday constant, C^* is the initial concentration of active materials in mol L^{-1}, ν is scan rate in V s^{-1}, A is electrode area in cm^2 (0.07 cm^2), and D is the diffusion coefficient in cm^2 s^{-1}.

From the anodic (upper) and cathodic (lower) peak currents of the $\mathbf{1}/\mathbf{1}^-$ couple, D values of 4.3×10^{-6} cm^2 s^{-1} (corresponding to $\mathbf{1}^-$) and 4.2×10^{-6} cm^2 s^{-1} (corresponding to **1**), respectively, are obtained. Similar analysis for the $\mathbf{1}^+/\mathbf{1}$ couple leads to D values of 3.6×10^{-6} cm^2 s^{-1} (anodic peaks, corresponding to **1**) and 4.3×10^{-6} cm^2 s^{-1} (cathodic peaks, corresponding to $\mathbf{1}^+$), respectively. Thus all species have diffusion coefficients on the order of 4×10^{-6} cm^2 s^{-1}, which is typical to other organic active species used in symmetric redox flow batteries in acetonitrile, such as diaminoanthroquinone **C** (~1×10^{-6} to ~5×10^{-7} cm^2 s^{-1}) [16], monomeric nitronyl nitroxide **A** (~6×10^{-6} cm^2 s^{-1}) [14], and ethylene glycol-linked bis(nitronyl nitroxide) **B** (~1×10^{-5} to ~5×10^{-6} cm^2 s^{-1}) [15], indicating suitability for testing in a battery.

3.2. Charge–discharge tests

We subsequently investigated the charge–discharge performance in a non-flowing cell, initially assembled in the discharged state with 0.04 M **1** in 0.5 M $TBAPF_6$ in CH_3CN as both anode- and cathode-active solutions (theoretical capacity of 1.07 Ah L^{-1}). This low concentration was chosen to ensure good solubility of the active material in all three charge states. The cell employed an AHA anion exchange membrane to separate the two electrodes and employed graphitic carbon felt as current collectors. Charging and discharging were conducted at a relatively low current density of 0.12 mA cm^{-2} (corresponding to a theoretical charge/discharge time of 1 h) in order to achieve acceptable voltage efficiencies, with upper and lower cut-off voltages of 1.6 and 0.5 V, respectively, for 50 cycles. During the first cycle (Fig. 4a), the cell exhibited an average charging and discharging voltage of 1.16 and 0.79 V, respectively (voltage efficiency (VE) of 68%), with a cell potential of 0.97 V, which is close to the value expected based on CV analysis (0.98 V). Of the theoretical charge, 98% and 93%, respectively, were utilized during charging and discharging, with an initial coulombic efficiency (CE) of 94%, giving an energy efficiency (EE) of 64% for the first cycle. Despite the inherently disadvantageous diffusion of active materials to the electrode surface in a non-flowing cell compared to flow-cell conditions [15], the high initial utilization of active materials and coulombic efficiencies for the test cell featuring **1** are noteworthy among other symmetrical RFBs featuring organic active materials. For example, a static cell employing ethylene glycol-linked nitronyl nitroxides **B** led to only 27% of theoretical discharge capacity in the first cycle at 1 mA cm^{-2}, with an initial CE of ~55% [15], while a non-flowing cell based on a diaminoquinone **C** showed only 80% CE initially [16]. Considering the observed discharge voltage, and the realization of 93% of the theoretical discharge, the energy density for the first discharge was 0.39 Wh L^{-1}, which is 75% of the theoretical value of 0.52 Wh L^{-1}. Though the VE remained quite steady throughout the experiment, and an average CE of 96% was demonstrated, the charging and discharging capacities dropped steadily to only about 31% of the theoretical value by cycle 50 (Fig. 4b). It is notable that, despite the

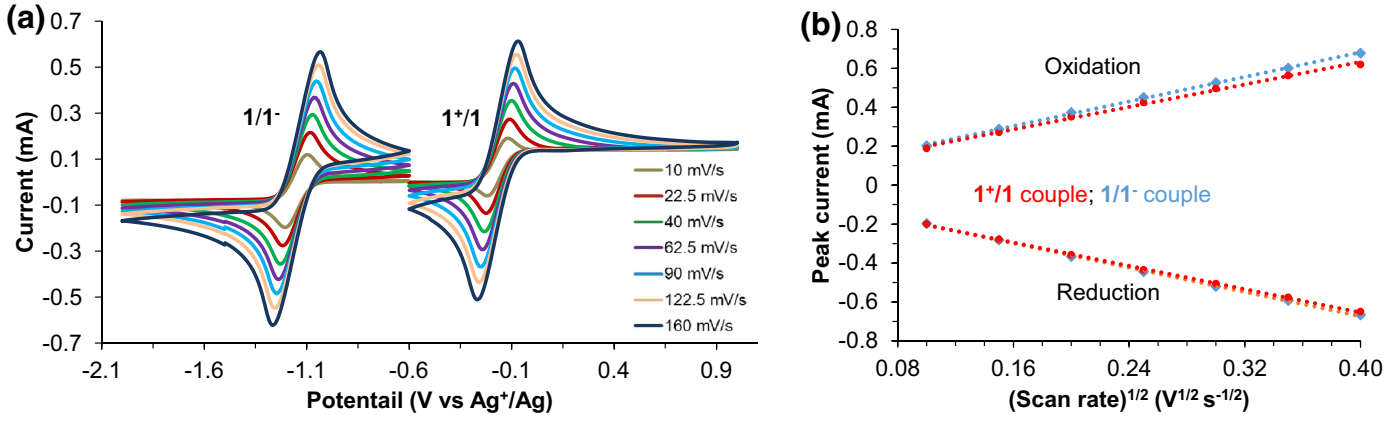

Fig. 3. (a) CV curves of **1** in 0.5 M $TBAPF_6/CH_3CN$ at varying scan rates; (b) plots of the oxidation and reduction peak currents for each of the redox couples vs. the square root of the scan rate.

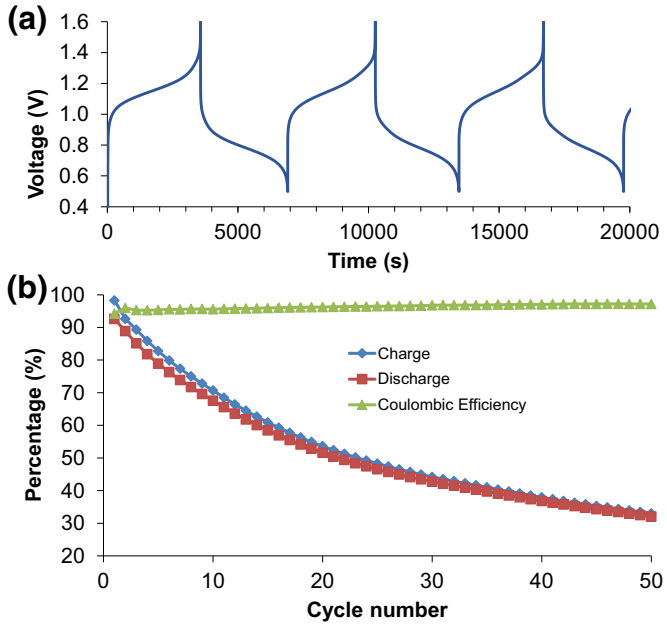

Fig. 4. (a) Charge and discharge curves for the first 3 cycles of a symmetric non-flowing RFB with 0.04 M **1** in 0.5 M $TBAPF_6/CH_3CN$ as both catholyte and anolyte; (b) plots of the charging and discharging capacities (as percent of theoretical 1.07 Ah L^{-1}) and coulombic efficiency for each cycle.

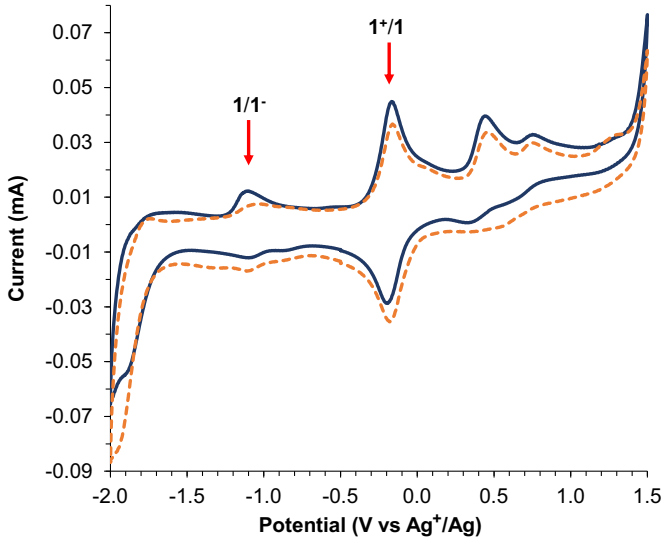

Fig. 5. CV curves of the anolyte (solid dark blue line) and catholyte (dashed orange line) side of a symmetric RFB based on 0.04 M **1** in 0.5 M $TBAPF_6/CH_3CN$ after 26 charge/discharge cycles. (For interpretation of the references to color in this figure legend, the reader is referred to the web version of this article.)

fact that the neutral and anionic forms of the verdazyl can theoretically pass through the anion exchange membrane, the high first discharge capacity signifies that it is effective in minimizing unwanted crossover.

With a new cell, the cell cycling was repeated as before, with the exception that the experiment was halted after 26 charge/discharge cycles. The cell was subsequently disassembled and the electrolyte from the carbon felts of both catholyte and anolyte sides of the cell were extracted into fresh electrolyte for CV analysis. The results show that **1** is still present in both sides of the cell (Fig. 5, red arrows), but some new unidentified electrochemically active species have been generated, as indicated by oxidation peaks at around 0.4 and 0.7 V vs Ag^+/Ag. It is noted that the anolyte and catholyte sides look qualitatively similar, though the signals for the $\mathbf{1}/\mathbf{1}^-$ couple are greatly diminished relative to the $\mathbf{1}^+/\mathbf{1}$ couple. This suggests that decomposition products are interacting or reacting with the anion more than the neutral species or cation, and that the anion is primarily responsible for the decomposition process. Although mechanistic studies will be needed to shed further understanding, it is clear that the active material is decomposing with cycling and this is the primary cause of capacity fade in the symmetric RFB.

4. Conclusions

A symmetrical, static battery employing acetonitrile solutions of 3-phenyl-1,5-di-*p*-tolylverdazyl (**1**) as both catholyte and anolyte-active species has been proposed and investigated. Randles–Sevcik analysis of cyclic voltammetric data on an electrolyte of 0.04 M **1** in 0.5 M $TBAPF_6/CH_3CN$, demonstrated chemically reversible redox processes and suitable diffusion coefficients on the order of 4×10^{-6} cm^2 s^{-1} for all three states of charge. In charge–discharge testing, the symmetric cell showed a cell voltage of 0.97 V and very high utilization of active materials for the initial charge (98%) and discharge (93%), but the available capacity deteriorated to ~30% by the 50th charge. Analysis of the cycled electrolyte showed that decomposition of the anionic species is likely the major cause for the loss of performance in cycling.

Nevertheless, the promising results of the first cycle warrant further investigation on verdazyl systems for energy storage. Future work should target modifications to the parent scaffold that allow for higher solubility, and a widening of the potential gap between the oxidation and reduction of the radical. Both will favorably increase the energy density, which was limited in this study. Additionally, efforts to minimize the decomposition of the verdazyl species on cycling, either through structural modification and/or altering the electrolyte salt or solvent, will be key to increasing the cycle life. Such modifications are an established advantage of organic systems that allows for improved cell performance [23–26].

Acknowledgments

This work was supported by the Natural Sciences and Engineering Research Council (NSERC) of Canada (C. A. D.: DG, 04279; J. B. G.: DG, 435675 and S. M. B.: CGS D scholarship). C. A. D. is also grateful to support form the Canada Foundation for Innovation (CFI) the New Brunswick Innovation Foundation (NBIF), and the University of New Brunswick. J. B. G. would like to thank the University of Western Ontario for support.

Supplementary materials

Supplementary material associated with this article can be found, in the online version, at doi:10.1016/j.jechem.2018.09.020.

References

[1] P. Leung, X. Li, C. Ponce De León, L. Berlouis, C.T.J. Low, F.C. Walsh, RSC Adv. 2 (2012) 10125–10156.
[2] F. Díaz-González, A. Sumper, O. Gomis-Bellmunt, R. Villafáfila-Robles, Renew. Sustain. Energy Rev. 16 (2012) 2154–2171.
[3] G.L. Soloveichik, Annu. Rev. Chem. Biomol. Eng. 2 (2011) 503–527.
[4] P. Alotto, M. Guarnieri, F. Moro, Renew. Sustain. Energy Rev. 29 (2014) 325–335.
[5] Y. Zhao, Y. Ding, Y. Li, L. Peng, H.R. Byon, J.B. Goodenough, G. Yu, Chem. Soc. Rev. 44 (2015) 7968–7996.
[6] T. Janoschka, N. Martin, U. Martin, C. Friebe, S. Morgenstern, H. Hiller, M.D. Hager, U.S. Schubert, Nature 527 (2015) 78–81.
[7] J. Noack, N. Roznyatovskaya, T. Herr, P. Fischer, Angew. Chem. Int. Ed. 54 (2015) 9776–9809.
[8] G.L. Soloveichik, Chem. Rev. 115 (2015) 11533–11558.
[9] M. Skyllas-Kazacos, L. Cao, M. Kazacos, N. Kausar, A. Mousa, ChemSusChem 9 (2016) 1521–1543.

[10] Á. Cunha, J. Martins, N. Rodrigues, F.P. Brito, Int. J. Energy Res. 39 (2015) 889–918.
[11] J. Winsberg, T. Hagemann, T. Janoschka, M.D. Hager, U.S. Schubert, Angew. Chem. Int. Ed. 56 (2017) 686–711.
[12] H. Chen, G. Cong, Y.C. Lu, J. Energy Chem. 27 (5) (2018) 1304–1325.
[13] X. Wei, W. Pan, W. Duan, A. Hollas, Z. Yang, B. Li, Z. Nie, J. Liu, D. Reed, W. Wang, V. Sprenkle, ACS Energy Lett. 2 (2017) 2187–2204.
[14] W. Duan, R.S. Vemuri, J.D. Milshtein, S. Laramie, R.D. Dmello, J. Huang, L. Zhang, D. Hu, M. Vijayakumar, W. Wang, J. Liu, R.M. Darling, L. Thompson, K. Smith, J.S. Moore, F.R. Brushett, X. Wei, J. Mater. Chem. A 4 (2016) 5448–5456.
[15] T. Hagemann, J. Winsberg, B. Häupler, T. Janoschka, J.J. Gruber, A. Wild, U.S. Schubert, NPG Asia Mater. 9 (2017) e340.
[16] R.A. Potash, J.R. McKone, S. Conte, H.D. Abruña, J. Electrochem. Soc. 163 (2016) A338–A344.
[17] K.H. Hendriks, C.S. Sevov, M.E. Cook, M.S. Sanford, ACS Energy Lett. 2 (2017) 2430–2435.
[18] S.H. Oh, C.W. Lee, D.H. Chun, J.D. Jeon, J. Shim, K.H. Shin, J.H. Yang, J. Mater. Chem. A 2 (2014) 19994–19998.
[19] J. Winsberg, C. Stolze, S. Muench, F. Liedl, M.D. Hager, U.S. Schubert, ACS Energy Lett. 1 (2016) 976–980.
[20] T. Janoschka, C. Friebe, M.D. Hager, N. Martin, U.S. Schubert, ChemistryOpen 6 (2017) 216–220.
[21] J.B. Gilroy, S.D.J. McKinnon, B.D. Koivisto, R.G. Hicks, Org. Lett. 9 (2007) 4837–4840.
[22] A.J. Bard, L.R. Faulkner, Electrochemical Methods: Fundamentals and Applications, second ed., Wiley, New York, 2001.
[23] X. Wei, W. Xu, J. Huang, L. Zhang, E. Walter, C. Lawrence, M. Vijayakumar, W.A. Henderson, T. Liu, L. Cosimbescu, B. Li, V. Sprenkle, W. Wang, Angew. Chem. Int. Ed. 54 (2015) 8684–8687.
[24] L. Cheng, R.S. Assary, X. Qu, A. Jain, S.P. Ong, N.N. Rajput, K. Persson, L.A. Curtiss, J. Phys. Chem. Lett. 6 (2015) 283–291.
[25] C.S. Sevov, D.P. Hickey, M.E. Cook, S.G. Robinson, S. Barnett, S.D. Minteer, M.S. Sigman, M.S. Sanford, J. Am. Chem. Soc. 139 (2017) 2924–2927.
[26] Y. Ding, C. Zhang, L. Zhang, Y. Zhou, G. Yu, Chem. Soc. Rev. 47 (2018) 69–103.